An EXAFS study on oxidic and sulfided K–MoO_3/γ-Al_2O_3 catalysts

Guo-zhu Bian, Yil-lu Fu [1] and Ya-ning Xie [a]

Department of Chemical Physics, University of Science and Technology of China, Hefei, Anhui 230026, PR China
[a] *Institute of High Energy Physics, Chinese Academy of Science, Beijing 100039, PR China*

Received 23 October 1995; accepted 13 May 1996

By analyzing the extended X-ray absorption fine structure (EXAFS) of the Mo K-absorption edge, structural information for both oxidic and sulfided K–MoO_3/γ-Al_2O_3 catalysts with different potassium content was obtained. The oxidic samples show two backscatterer peaks in the radial distribution function (RDF), which correspond to the Mo–O coordinations in the nearest Mo–O shell. The nearest oxygen atoms are present with large configurational disorder. The RDF for the K/Mo = 0 sample is significantly different from that for crystalline MoO_3 and ammonium heptamolybdate. The RDFs for potassium promoted samples are, in some extent, similar to that for ammonium heptamolybdate. The sample with K/Mo = 0.8 and that with K/Mo = 1.5 do not show obvious difference in their local Mo–O structures. The EXAFS results support the earlier conclusions from Raman spectroscopy studies on identical samples [7]. When the samples are sulfided, a rearrangement of the local neighbors around Mo atoms takes place, to form small MoS_2-like crystallites. The Mo–S and Mo–Mo coordination distances on these catalysts are the same as those in crystalline MoS_2, but the coordination numbers are significantly lower than in MoS_2. The EXAFS results indicate that Mo species on the K/Mo = 0 catalyst mainly consist of Mo–S–Mo units (the basic building units of MoS_2), which are highly dispersed and show a higher level of disorder than in MoS_2. With the modification by the potassium promoter, Mo species are significantly aggregated and their local neighbors are more similar to those in MoS_2, but the Mo species still exist in a state of high dispersion.

Keywords: K–MoO_3/Al_2O_3 catalysts; oxidic and sulfided states; EXAFS; structure

1. Introduction

Sulfided Mo based catalysts have been widely used in hydrotreating processes because of their high activity for hydrodesulfurization, hydrodenitrogenation, methanation and synthesis of light hydrocarbons from CO hydrogenation [1]. In recent years, some attention has been focused on alkali, mainly potassium, promoted catalysts since they show high activity for mixed alcohols synthesis from CO hydrogenation [2–4]. As a promoter, K_2CO_3 has been used by some experimental groups in MoS_2 catalysts [1,5]. Some authors have claimed that KCl is the preferred promoter for the MoO_3/SiO_2 system [6].

Previously, we studied the role of KCl as promoter in MoO_3/γ-Al_2O_3 catalysts. For this purpose, a variety of techniques including X-ray diffraction (XRD) and laser Raman spectroscopy (LRS) were used to determine the structural features of the catalysts [7]. The results showed that for oxidic samples the main surface phase on the MoO_3/Al_2O_3 sample was MoO_3 crystallite, but the surface phase on KCl promoted samples was present mainly in the form of K–Mo interaction species, which may contain the potassium cations and the $Mo_7O_{24}^{6-}$ unit. For sulfided samples, MoS_2 crystallites were formed and the presence of the potassium promoter resulted in the aggregation of the MoS_2 crystallites. But questions remain about the local structure of Mo atoms on these catalysts.

[1] To whom correspondence should be addressed.

Extended X-ray absorption fine structure (EXAFS) probes the local environment of the absorber atoms and allows a determination of structural parameters such as coordination numbers and interatomic distances [8]. The local coordination of the catalytically active atoms could be expected to answer some questions relating to the molecular mechanism of the surface active species without long-range order.

Since the early 1980s, EXAFS has been used to characterize the structure of the surface species on both oxidic and sulfided Mo based catalysts. For oxidic catalysts, some authors have reported the results of EXAFS analysis about the influences on the structure of Mo species of supports [9], concentration of Mo component [10] and of pretreatment conditions [11]. Recently, Knözinger et al. have reported their results about the influences of a potassium promoter on the structure of the Mo species on oxidic SiO_2-supported samples [12]. Chiu et al. have reported the structure of Co–Mo/Al_2O_3 catalyst determined by EXAFS [13]. For sulfided catalysts, some studies concerning the influences on the structure of Mo species of sulfidation conditions [14] and Co- and Ni-containing promoters [15–19] have been reported. These EXAFS results suggest that Mo species on oxidic samples are often poorly ordered, but for Mo species on sulfided samples there is a higher level of microcrystalline order. Most results from EXAFS analysis are also supported by conclusions obtained from other techniques.

With the aim to obtain additional microstructural

information on our K–MoO_3/Al_2O_3 catalysts, we now report the results obtained from the study by EXAFS of the Mo K-absorption edge. In this paper, both the oxidic and sulfided samples were prepared under conditions identical to those applied in earlier studies [7].

2. Experimental

2.1. Sample preparation

The oxidic K–MoO_3/γ-Al_2O_3 samples were prepared, by the incipient wetness method, by impregnating γ-Al_2O_3 support with the aqueous solution of KCl (the solution for 1 g Al_2O_3 support was obtained by adding a calculated amount of KCl to 2 g distilled water), followed by drying in air at 120°C for 6 h and calcination in air at 300°C for 1 h; and then impregnating these KCl/γ-Al_2O_3 samples with the solution of ammonium heptamolybdate, followed by drying and calcination in O_2 atmosphere at 500°C for 12 h. The oxidic samples were sulfided by calcination at 400°C for 6 h in a flowing gas mixture (30 ml/min) of H_2 and CS_2, which was obtained by passing H_2 through 0°C liquid CS_2. Mo contents calculated as MoO_3/Al_2O_3 weight ratio are constant for all samples and equal to 0.24; potassium contents calculated as K/Mo atomic ratio are equal to 0, 0.8, 1.5, respectively. The sulfided samples were protected in N_2 atmosphere and only exposed to air for short time before the EXAFS measurements.

2.2. EXAFS analysis

X-ray absorption data around the Mo K-absorption edge were collected at the beamline of 4WIB, the EXAFS station of the Beijing Synchrotron Radiation Facility. The measurements were performed at room temperature with ionization chambers filled with Ar. For the EXAFS measurements, the samples were ground and homogenized. The precalculated amounts of samples were pressed into plane-parallel rectangular tablets and the reference compounds were mounted between pieces of adhesive tape. The thickness of the samples was chosen such that $\mu x = 1$ on the high absorption side of the edge. The X-rays, which were emitted by positrons in the storage ring with an energy of 2.2 GeV and a typical current of 45 mA, were monochromatized by two Si(111) single crystals. All spectra were obtained at 5 eV steps from 19800 to 19940 eV, 1 eV steps from 19940 to 20200 eV and 4 eV steps up to 21000 eV.

The EXAFS functions in k-space were obtained from the X-ray absorption spectra by successively subtracting the extrapolation of a victoreen curve fitted to the pre-edge region and a victoreen curve fitted to the post-edge region. Normalization was done by division by the apparent edge height, which is obtained by back extrapolation of the backgrounds. The k^3-weighted EXAFS functions were Fourier transformed (FT) over a k-range of 30–130 nm^{-1} to obtain the FT spectra. The FT spectra were inverse Fourier transformed over a certain R-range to obtain the isolated EXAFS functions in k-space. The R-range limits chosen were minima in the values of the spectra to minimize cutoff effects.

For the analysis of the spectra, phase shifts and backscattering amplitudes from reference compounds were used. For this purpose, we have employed $Na_2MoO_4 \cdot 2H_2O$ and MoS_2, and used the EXAFS results of Mo–O in $Na_2MoO_4 \cdot 2H_2O$ and Mo–S, Mo–Mo in MoS_2 as standards. The interatomic distance calculations have an uncertainty of about ±0.002 nm, and coordination number with about ±20% uncertainty for Mo–S shell and more for Mo–O and Mo–Mo shells.

3. Results and discussion

3.1. EXAFS analysis for model compounds and oxidic catalyst samples

The radial distribution functions (RDF) derived from the EXAFS of $Na_2MoO_4 \cdot 2H_2O$, MoO_3 and $(NH_4)Mo_7O_{24} \cdot 4H_2O$ are shown in fig. 1. Fig. 1a presents the radial distribution of $Na_2Mo_4 \cdot 2H_2O$, which contains only a single large peak at about 0.13 nm corresponding to the four nearest oxygen neighbors. The Mo–O distances are 0.176 nm according to literature [20]. The position of the peak on the RDF is downshifted from the

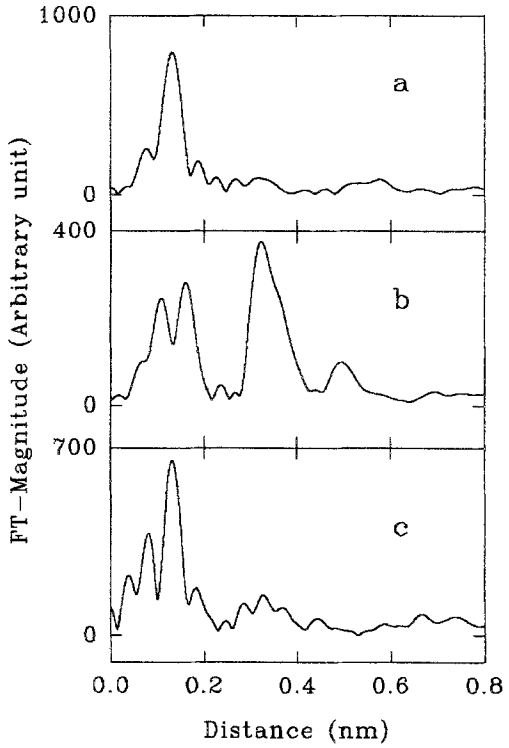

Fig. 1. Radial distribution functions for model oxidic Mo compounds. (a) $Na_2MoO_4 \cdot 2H_2O$, (b) MoO_3, (c) $(NH_4)_6Mo_7O_{24} \cdot 4H_2O$.

true distance by about 0.045 nm due to the scattering phase shifts. The sharpness of the Mo–O peak in the RDF implies that the Mo–O coordination shells are present with small configurational disorder.

Fig. 1b presents the RDF of crystalline MoO_3. In this figure, there are three major peaks. The first two peaks at about 0.12 and 0.18 nm correspond to six nearest neighbor oxygen atoms of the Mo atom. These six oxygens form a distorted octahedron. The Mo–O coordination distances are known as 0.165, 0.173, 0.195, 0.225 and 0.233 nm; the Mo–O coordination numbers are 1, 1, 2, 1 and 1, respectively [21]. The third large peak at about 0.29 nm on the RDF for MoO_3 is due to the next nearest neighbors, which contains two Mo atoms at about 0.344 nm, and four Mo and six O atoms that are present within distances shorter than 0.4 nm.

The first two peaks on the RDF for MoO_3 are weak compared to the first peak in $Na_2MoO_4{\cdot}2H_2O$. This is because of the large spread in the Mo–O distances of the first coordination shell of MoO_3, which reduces the apparent amplitude where the peaks are overlapping and makes a minimum [8]. The minimum between the nearest Mo–O peaks for MoO_3 is at about 0.15 nm. Recall that the peak position on the RDF is downshifted from the true distance by about 0.045 nm; this minimum position should be the maximum of a peak attributed to the two 0.195 nm Mo–O coordinations if the interference were not present. Knözinger et al. reported a similar radial distribution for MoO_3 [11].

The RDF for ammonium heptamolybdate is presented in fig. 1c. In this figure, one large peak at about 0.13 nm is observed, which corresponds to the Mo–O coordination with interatomic distances of near 0.18 nm. The small peak at about 0.18 nm on the RDF may represent the Mo–O coordination with longer Mo–O interatomic distances (near 0.23 nm). In the ammonium heptamolybdate unit cell, each Mo atom is surrounded by six oxygen atoms that also form a distorted octahedron. Each unit cell contains seven Mo atoms, hence 42 Mo–O bonds. The Mo–O distances are widely distributed in a range of about 0.16–0.25 nm [11]. The existence of a minimum between the Mo–O peak at about 0.13 nm and the Mo–O peak at about 0.18 nm in the RDF is also caused by the large configurational disorder and the interference of the Mo–O coordinations with different interatomic distances.

The inverse transforms of the nearest Mo–O peaks of the model compounds were calculated. These were fitted to find the Mo–O coordination of MoO_3 and ammonium heptamolybdate, using the inverse transform of $Na_2MoO_4{\cdot}2H_2O$ as a standard. When the two nearest Mo–O peaks in the RDFs for MoO_3 or ammonium heptamolybdate were inversely transformed separately, the single-shell fitting showed much lower coordination numbers (1.4 and 1.6) compared to the crystallographic number (6). When the two peaks were inversely transformed together, the results from two-shell fitting are in good agreement with the crystallographic parameters (see table 1). The average Mo–O coordination distances in ammonium heptamolybdate from EXAFS analysis were a little longer than in MoO_3.

Fig. 2 shows the RDFs derived from the EXAFS data of oxidic samples with different potassium contents. On each RDF there are two peaks in the range of 0.10–0.22 nm, one at about 0.13 nm and another at 0.18 nm. They correspond to the nearest Mo–O shells in the samples. These peaks are notably decreased compared to that for $Na_2MoO_4{\cdot}2H_2O$, which suggests that Mo species on the oxidic samples are presented with large configurational disorder [22,23].

In fig. 2a, the RDF for the oxidic K/Mo = 0 sample, the Mo–O peak at about 0.18 nm is smaller than the peak at about 0.13 nm. Recall that the peak due to more distant oxygen neighbors in the nearest shell of crystalline MoO_3 is large and the second peak for ammonium heptamolybdate is much smaller. The local structure around Mo atoms on the K/Mo = 0 sample should be different from either MoO_3 or ammonium heptamolybdate. We have reported that on this sample strong bands due to MoO_3 and weak bands due to some tetrahedral and octahedral Mo species were observed by laser Raman spectroscopy [7], which suggested that a mixture of several different Mo species is present in the sample. This is in agreement with the results from EXAFS analysis. Another significant difference between the radial distribution functions for the K/Mo = 0 sample and for crystalline MoO_3 is that the peaks at about 0.28 nm (corresponding to Mo–Mo and farther Mo–O coordinations) for the K/Mo = 0 sample are small relative to those for crystalline MoO_3. This indicates that the MoO_3-like species on the K/Mo = 0 sample may be present as MoO_3, but lacking the long-range order characteristics of crystalline MoO_3. This is consistent with XRD [7], by which no peaks were found due to any Mo species, although the Mo content on this sample was about 20%.

The inverse transforms were calculated for the nearest Mo–O shell on the oxidic samples, and two-shell fitting

Table 1
Best-fit values of structural parameters for oxidic samples from EXAFS data

Sample		Shell	N	R (nm)
MoO_3		Mo–O	3.0	0.176
		Mo–O	3.0	0.223
$(NH_4)_6Mo_7O_{24}{\cdot}4H_2O$		Mo–O	2.3	0.189
		Mo–O	3.4	0.235
K/Mo	0.0	Mo–O	3.0	0.178
		Mo–O	2.1	0.218
	0.8	Mo–O	2.2	0.180
		Mo–O	2.8	0.238
	1.5	Mo–O	2.2	0.181
		Mo–O	2.7	0.238

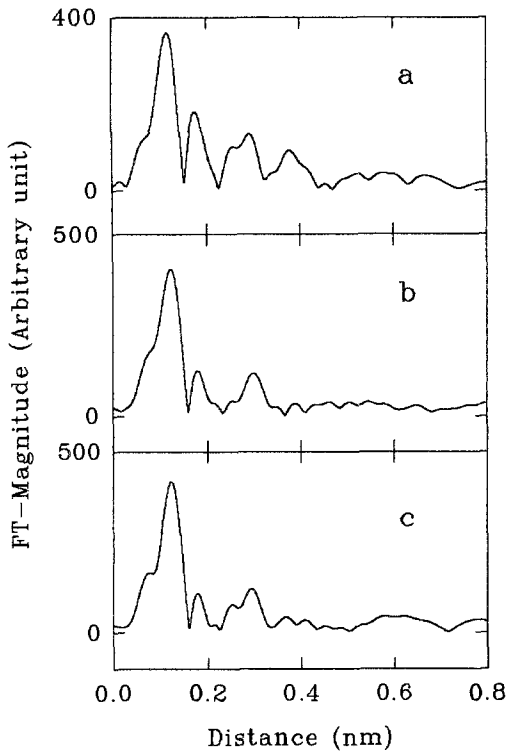

Fig. 2. Radial distribution functions for oxidic K–MoO_3/Al_2O_3 samples. (a) K/Mo = 0.0, (b) K/Mo = 0.8, (c) K/Mo = 1.5.

of the inverse transforms was performed. Fig. 4a shows the inverse transformation spectra and fits, for the nearest Mo–O shell of the K/Mo = 0 sample. The structural parameters from the fitting are included in table 1. The two Mo–O coordination distances for the K/Mo = 0 sample are both shorter than their counterparts for K-promoted samples. Compared to the other samples, the Mo–O coordination distances for the K/Mo = 0 sample and for crystalline MoO_3 are short. The Mo–O coordination distances for K-promoted samples, ammonium heptamolybdate and $Na_2MoO_4 \cdot 2H_2O$ are relatively longer. These results support the idea that a part of the Mo component in the K/Mo = 0 sample is present as MoO_3 crystallites.

In figs. 2b and 2c, the radial distribution functions for K/Mo = 0.8 and K/Mo = 1.5 samples are presented. The results of two-shell fitting do not show significant differences in local Mo–O structures between the sample with K/Mo = 0.8 and the sample with K/Mo = 1.5. The peaks due to longer Mo–O coordinations (at about 0.18 nm) in the nearest shells of these two samples are both much weaker. Parham et al. reported similar radial distribution functions for oxidic Mo catalysts [14]. The RDFs for the K-promoted samples are similar to that for ammonium heptamolybdate, which are consistent with the results obtained from LRS measurements that MoO_3 crystallites disappeared and some $Mo_7O_{24}^{6-}$ species formed on the K-promoted samples [7]. The structural parameters from EXAFS fitting supported this idea, which showed that Mo–O coordination distances in the K-promoted samples are a little longer than in the K/Mo = 0 sample. But the existence of K promoter, and some tetrahedral Mo species which has been observed by LRS [7], imply the local Mo–O structures must have some difference from that in ammonium heptamolybdate.

According to LRS and XRD analysis [7], on oxidic potassium-promoted samples an interaction between the potassium promoter and the supported molybdenum component occurs. The K–Mo interaction gets saturated by a K/Mo ratio of 0.8. At a K/Mo ratio above 0.8, KCl crystallites form. These conclusions are in agreement with the results from EXAFS analysis.

3.2. *EXAFS analysis for sulfided K–MoO_3/Al_2O_3 samples*

The RDF for MoS_2 is presented in fig. 3a. In this figure, there are two large peaks. The first peak at about 0.19 nm corresponds to six sulfur neighbors at 0.241 nm. The second large peak at about 0.28 nm is caused by six Mo neighbors at 0.316 nm [24], which make up the first Mo–Mo shell. The peaks which represent more distant S

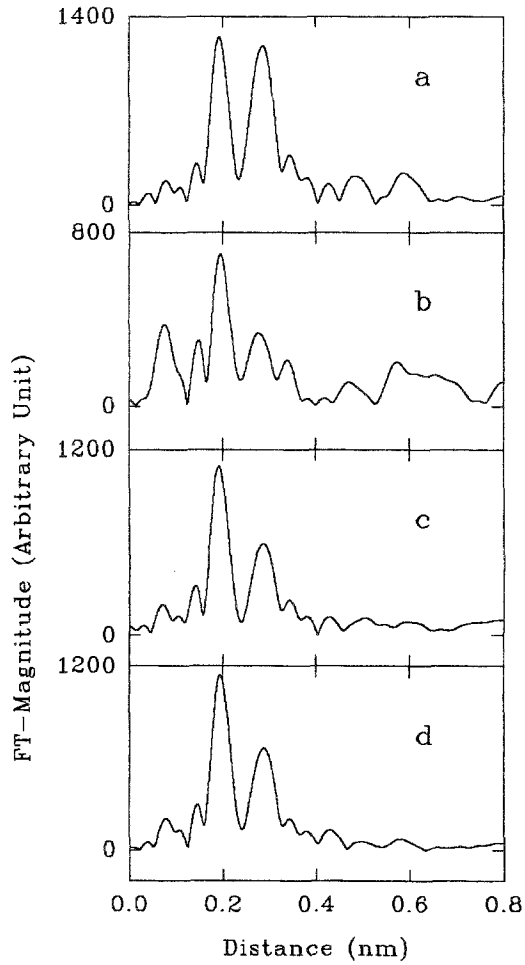

Fig. 3. Radial distribution functions for MoS_2 and sulfided K–MoO_3/Al_2O_3 samples. (a) MoS_2, (b) K/Mo = 0.0, (c) K/Mo = 0.8, (d) K/Mo = 1.5.

and Mo shells are much smaller. The sharpness of the Mo–S peak and the Mo–Mo peak implies that S atoms and Mo atoms in the first Mo–S and Mo–Mo shells possess low configurational disorder.

The RDF for the sulfided sample with K/Mo = 0 is presented in fig. 3b. In this figure, there are also two major peaks due to Mo–S and Mo–Mo coordination shells, respectively. Both the Mo–S and Mo–Mo distances on this sample are in agreement with the interatomic distances in MoS_2. This indicates that organization into MoS_2-like crystallites took place during sulfidation. One obvious difference compared to the RDF of MoS_2 is that the magnitudes of the Mo–S and Mo–Mo peaks for the sulfided sample are small relative to those for MoS_2. and also that the Mo–Mo peak is much smaller than the Mo–S peak. This implies a lower Mo–S coordination number and a much lower Mo–Mo coordination number in the sulfided K/Mo = 0 sample. Figs. 3c and 3d present the RDFs for the sulfided catalyst samples with K/Mo = 0.8 and K/Mo = 1.5. The local structures of these samples are similar to the K/Mo = 0 sample except that the heights of both the Mo–S peak and Mo–Mo peak are increased.

The structural parameters of Mo–S and Mo–Mo coordination shells for the sulfided catalysts were obtained by single-shell fitting of the inverse transformation data. The calculated values are included in table 2. The Mo–S and Mo–Mo coordination distances do not show obvious differences from MoS_2, but the coordination numbers, especially the Mo–Mo coordination numbers, are much smaller than those of MoS_2. Figs. 4b and 4c present the inverse transformation spectra of Mo–S and Mo–Mo shells in the MoS_2 (curve 1) and K/Mo = 0.8 samples (curve 2), and the final fit for the spectrum of the K/Mo = 0.8 sample (dotted), respectively.

In table 2, for the K/Mo = 0 sample, the Mo–S coordination number is 3.7 according to EXAFS analysis. Total sulfur analysis showed, however, that S/Mo atomic ratios on similar samples are less than 2 [25,26]. These results indicate that most of sulfur atoms in the sample should be coordinated with approximately two Mo atoms, which demonstrates clearly that the Mo species on the sample are present in the form of a chain-like structure with Mo–S–Mo bonds as basic building units. The much smaller value of the Mo–Mo coordination

Table 2
Best-fit values of structural parameters for sulfided catalysts from EXAFS data

Sample		Shell	N	R(nm)
K/Mo	0.0	Mo–S	3.7	0.244
		Mo–Mo	1.4	0.313
	0.8	Mo–S	5.0	0.240
		Mo–Mo	3.4	0.316
	1.5	Mo–S	5.0	0.242
		Mo–Mo	3.6	0.317

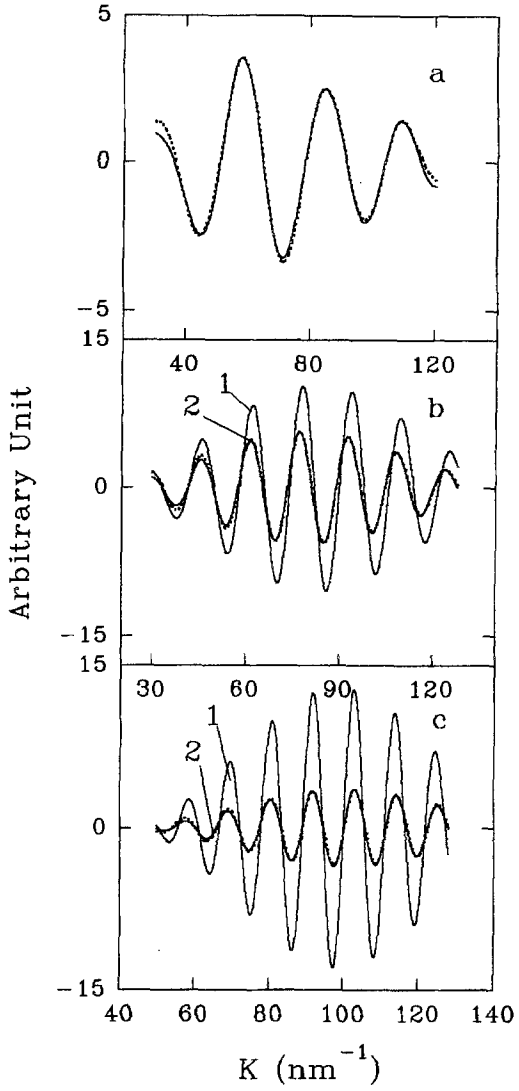

Fig. 4. Inverse transformation spectra and the final fits with the parameters as presented in tables 1 and 2. (——) Experimental curve, (···) fitting curve. (a) Mo–O shell in oxidic K/Mo = 0 sample, (b) Mo–S shell in MoS_2 (1) and K/Mo = 0.8 sample (2), (c) Mo–Mo shell in MoS_2 (1) and K/Mo = 0.8 sample (2).

number from EXAFS analysis (1.4) suggests a high level of disorder of the Mo–Mo coordination. So, the arrangement of Mo–S–Mo units on the catalyst sample should be structurally different from MoS_2, in which the Mo–S–Mo units (the basic building units of MoS_2) are present with lower configurational disorder and each sulfur atom is coordinated with three Mo atoms. Small crystallites of MoS_2 on the sample surface would readily explain this effect.

Significant structural changes for the K-promoted catalyst samples compared to the K/Mo = 0 sample are observed from the EXAFS measurement (table 2). The Mo–S coordination number for the K/Mo = 0.8 sample is 5.1, which is higher than the value (3.7) for the K/Mo = 0 sample. This implies that an aggregation of the Mo species occurs during sulfidation on the K/Mo = 0.8 sample. The increase of the Mo–Mo coor-

dination number (3.4) for the K/Mo = 0.8 sample compared to that for the K/Mo = 0 sample (1.4) supports this idea. So, the local arrangement of the Mo species on the K/Mo = 0.8 sample is more similar to that in MoS_2. In the K/Mo = 1.5 sample, the Mo–S coordination number is 5.0 and Mo–Mo coordination number is 3.6. No evidence is seen for significant structural changes compared to the K/Mo = 0.8 sample. This suggests that similar structural rearrangements occur on these two K-promoted samples during sulfidation.

All of these results indicate that the size of the MoS_2 crystallites increases when catalysts are promoted with the potassium compound. This is in agreement with the results obtained from LRS measurements [7]. In the Raman spectra, obvious scattering peaks corresponding to MoS_2 were observed for K-promoted catalysts, while no obvious signals were observed for the K/Mo = 0 sample.

4. Conclusion

By analyzing the EXAFS of the Mo K-absorption edge, we know that for oxidic K–MoO_3/Al_2O_3 catalysts the nearest oxygen atoms are present with large configurational disorder. The radial distribution function for the K/Mo = 0 sample is significantly different from that for MoO_3 and ammonium heptamolybdate. The Mo species on these samples are present as a mixture of MoO_3 crystallite. and some other Mo species. The local structures on K-promoted samples are similar to those in ammonium heptamolybdate. The samples with K/Mo = 0.8 and K/Mo = 1.5 do not show obvious difference between them in their local Mo–O structures. When the catalysts are sulfided, a rearrangement of the local neighbors takes place around Mo atoms to form MoS_2-like crystallites. The Mo–S and Mo–Mo coordination distances on these catalysts are the same as in MoS_2, but the coordination numbers are significantly lower. The EXAFS results indicate that Mo in the K/Mo = 0 sample mainly consists of Mo–S–Mo bonds (the basic building units of MoS_2), which are highly dispersed and possess a high level of disorder. With the modification by the potassium promoter, Mo species are significantly aggregated and their local neighbours are a little more similar to MoS_2.

Acknowledgement

This work was supported by National Natural Science Foundation of China. The experimental equipment was supplied by Beijing Synchrotron Radiation Facility. We greatly thank Professor Kun-quan Lu for supplying the calculation program and vice Professor Sho-qiang Wei for helpful discussion of the EXAFS analysis.

References

[1] M. Saito and R.B. Anderson, J. Catal. 63 (1980) 438.
[2] Y.C. Xie, B.M. Naase and G.A. Somorjai, Appl. Catal. 27 (1986) 223.
[3] C.B. Murchison, M.M. Conway, R.R. Stavens and G.J. Quarderer, in: *Proc. 9th Int. Congr. on Catalysis*, Vol. 2, eds. M.J. Phillips and M. Ternan, Calgary 1988 (Chemical Institute of Canada, Ottawa, 1988) p. 626.
[4] J.G. Santiesteban, C.E. Bogdan, R.G. Herman and K. Klier, in: *Proc. 9th Int. Congr. on Catalysis*, Vol. 2, eds. M.J. Phillips and M. Ternan, Calgary 1988 (Chemical Institute of Canada, Ottawa, 1988) p. 561.
[5] H.C. Woo, J.C. Kim, I.S. Nam, J.S. Lee et al., Appl. Catal. A 104 (1993) 199.
[6] T. Tatsumi, A. Muramatsu and H. Tominaga, Appl. Catal. 34 (1987) 77.
[7] M. Jiang, G.Z. Bian and Y.L. Fu, J. Catal. 146 (1994) 144.
[8] D.C. Koningsberger and R. Prins, eds., *X-ray Absorption: Principles and Techniques of EXAFS, SEXAFS and XANES* (Wiley, New York, 1989).
[9] H. Shimada, N. Matsubayashi, T. Sato, Y. Yoshimura and A. Nishijima, J. Catal. 138 (1992) 746.
[10] C.T.J. Mensch, J.A.R. van Veen, B. van Wingerden and M.P. van Dijk, J. Phys. Chem 92 (1988) 4961.
[11] G. Kisfaludi, J. Leyrer, H. Knözinger and R. Prins, J. Catal. 130 (1991) 192.
[12] N.F.D. Verbruggen, L.M.J.V. Hippel, G. Mestl, B. Lengeler and H. Knözinger, Langmuir 10 (1994) 3073.
[13] N.S. Chiu, S.H. Bauer and M.F.L. Johnson, J. Catal. 89 (1989) 226.
[14] T.G. Parham and R.P. Merrill, J. Catal. 85 (1984) 295.
[15] B.G. Clausen, H. Topsøe, R. Candia and J. Villadsen, J. Phys. Chem. 65 (1981) 3868.
[16] M.W.J. Craje, S.P.A. Louwers, V.H.J. Beer, R. Prins and A.M. van der Kraan, J. Phys. Chem. 96 (1992) 5445.
[17] N.S. Chiu, S.H. Bauer and M.F.L. Johnson, J. Catal. 98 (1986) 32.
[18] M.F.L. Johnson, A.P. Voss, S.H. Bauer and N.S. Chiu, J. Catal. 98 (1986) 51.
[19] A.S. Bommannavar and P.A. Montano, Appl. Surf. Sci. 19 (1984) 250.
[20] L.O. Atovmyan and O.A.D. Yackenko, J. Struct. Chem. 10 (1969) 504.
[21] L. Kihlborg, Ark. Kemi 21(34) (1963) 357.
[22] F. Comin, J.E. Rowe and P.H. Citrin, Phys. Rev. Lett. 51 (1983) 2402.
[23] E.A. Stern, P. Livins and Z. Zhang, Phys. Rev. B 43 (1991) 8850.
[24] R.G. Dickison and L.J. Pauling, Am. Chem. Soc. 45 (1923) 1466.
[25] Y.L. Fu, X.B. Tang, Z.G. Huang and C.Z. Fan, Appl. Catal. 55 (1989) 11.
[26] S.I. Kim and S.I. Woo, Appl. Catal. 74 (1991) 109.